第29卷 第6期
2005年6月

高 能 物 理 与 核 物 理
HIGH ENERGY PHYSICS AND NUCLEAR PHYSICS

Vol.29, No.6
Jun., 2005

Performance Study for Two Prototypes of Small-cell Drift Chamber with Different Cell Sizes

LIU Jian-Bei[1,2,1)] CHEN Chang[1] CHEN Yuan-Bo[1] JIN Yan[1] LIU Rong-Guang[1]
MA Xiao-Yan[1] MA Yuan-Yuan[1] QIN Zhong-Hua[1,2] TANG Xiao[1] WANG Lan[1]
WU Ling-Hui[1,2] XU Mei-Hang[1] ZHU Min-Xuan[1] ZHU Qi-Ming[1]

1 (Institute of High Energy Physics, CAS, Beijing 100049, China)
2 (Graduate School of the Chinese Academy of Sciences, Beijing 100049, China)

Abstract The spatial resolution, dE/dx resolution and cell efficiency of two prototypes of small-cell drift chamber filled with He/C_3H_8(60/40) with cell sizes of 14.0mm and 16.4mm were measured using cosmic rays respectively. The results show that the performances of the two drift chambers are almost equivalent.

Key words drift chamber, small cell, cell size

1 Introduction

The physics goals of BESⅢ[2)] experiment at the upgrading Beijing Electron-Positron Collider(BEPCⅡ)[3)] are precise measurements and the search for new physics in the tau-charm energy region. The drift chamber for BESⅢ is used to track charged particles produced in the electron-positron collisions, measure their momenta with magnetic field and their energy loss (dE/dx) for particle identification. The main requirements for the drift chamber are good efficiency, high momentum resolution, good dE/dx resolution and excellent adaptability for high event rate. These requirements are met by using a small cell chamber for the BESⅢ drift chamber and choosing the helium based gas of He/C_3H_8(60/40) for operation[2)]. In order to study the impact of cell size on the performance of the small-cell drift chamber filled with He/C_3H_8(60/40), we built two prototypes of drift chamber with different size cells in square shape and carried out a test using cosmic rays. The cell sizes are 14.0mm which has been adopted by the CLEO-Ⅲ drift chamber[1], and 16.4mm which is very similar to the BESⅢ drift chamber's final design[1], respectively.

In this work, we present the test results of the two prototype chambers including the spatial resolution, the dE/dx resolution and the cell efficiency. The performances of the two test chambers are also compared with each other.

2 Test chambers

The two prototype drift chambers are identical except for the cell size and the wire layers. One test chamber contains 10 layers of 5 cells each, with the cell size of 14.0mm (prototype 14.0). The other one contains 14 layers of 5 cells each, with the cell size of 16.4mm (prototype16.4). All the cells have standard square shapes to simplify the drift distance-time calibration. Each cell has one sense wire surrounded by a square grid of 8 field wires. The sense wires are 25μm diameter gold-plated tungsten (3% Re). The field wires are 110μm diameter gold-plated aluminum. The wires are about 60 cm long. All layers are axial with half cell staggering between neighbouring layers for left-right ambiguity

Received 9 December 2004

1) E-mail: liujb@mail.ihep.ac.cn

2) BESⅢ Preliminary Design Report. 2004

3) BEPCⅡ Preliminary Design Report. 2002

resolution. Fig.1 shows a close-up view of the wire configuration.

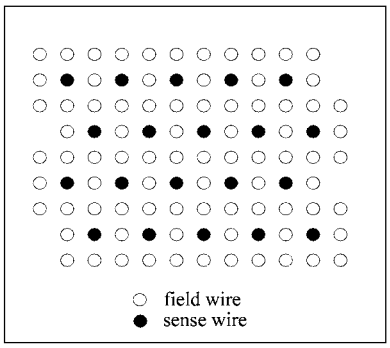

Fig.1. Wire configuration of the test chambers.

The high voltage is applied to the sense wires at one end-plate, while the preamplifier boards are mounted on the other end-plate. The field wires are all at ground potential. The two chambers were tested with He/C_3H_8(60/40) using cosmic rays. The test setup and electronics have been described in detail in Ref.[2].

3 Results

3.1 Drift distance-time relation

The drift distance-time relations (x-t relation) for the two test chambers are shown in Fig.2. The x-t relations are nonlinear. This is one significant character of the small cell which is caused by the nonuniform electric field in the cell inherent in its geometry. The x-t relation for the prototype 14.0 is consistent with the one for the prototype 16.4 in the whole drift cell except for the cell boundary where the electron's drift suffers from the distortion of the electric field. It should be noted that the x-t relation depends heavily on the operating voltage. The test shows that the x-t relations for the two chambers with He/C_3H_8(60/40) both will be improved on the nonlinearity with the increase of the operating voltage.

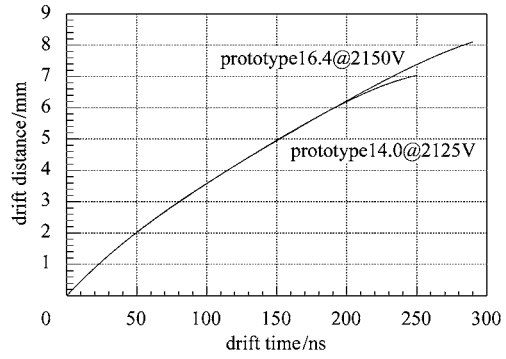

Fig.2. x-t relations for the two test chambers.

3.2 Spatial resolution

The spatial resolution as a function of distance from the sense wire for the two chambers is shown in Fig.3. The spatial resolution deteriorates near the sense wire because of the primary ionization statistics. The degradation near the cell edge is due to the distortion of the electric field. The two prototype chambers show a similar distance dependence of the spatial resolution.

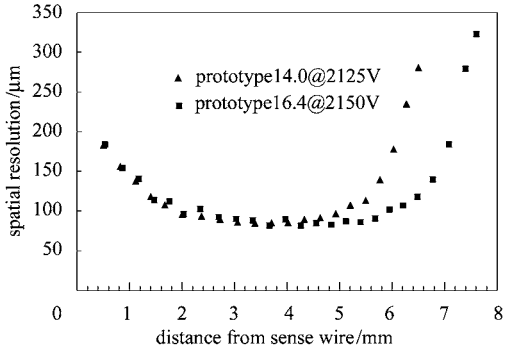

Fig.3. The spatial resolution as a function of distance from sense wire.

To compare the spatial resolution of the two test chambers, the gas gain is used as the operation condition rather than the operating voltage since the cell sizes of the two chamber are different. In practice, the gas gain is replaced by the relative gas gain, which is defined as the ratio of the peak of the pulse height spectrum to the path length in one cell. Fig.4 shows the dependence of the spatial resolutions of the two test chambers on the relative gas gain. The behaviors of the spatial resolutions due to the relative gas gain are similar. The spatial resolutions are improved significantly with the in-

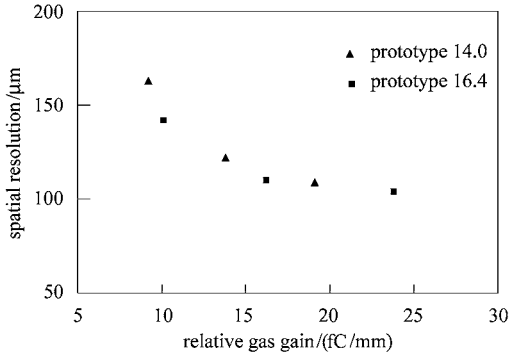

Fig.4. The dependence of the spatial resolution on the relative gas gain.

crease of the relative gas gain, i.e. the operating voltage and then arrive at a plateau with a resolution of about 100μm. The two chambers achieve almost equal spatial resolutions with the same gas gain.

3.3 dE/dx resolution

The truncated mean technique[3] is applied for the dE/dx measurement. Here only a fraction (truncation fraction) of the measured samples are used to calculate the dE/dx. The measured samples are ordered according to their pulse heights with the lowest f%(i.e. truncation fraction) of the samples used for the calculation. This procedure converts a landau spectrum into a Gaussian-like spectrum. The dE/dx resolution is then defined as the ratio of the width of the Gaussian to the peak.

The dE/dx resolution as a function of the truncation fraction for the two chambers is shown in Fig.5. The resolution has a broad minimum near the truncation fraction of 60%.

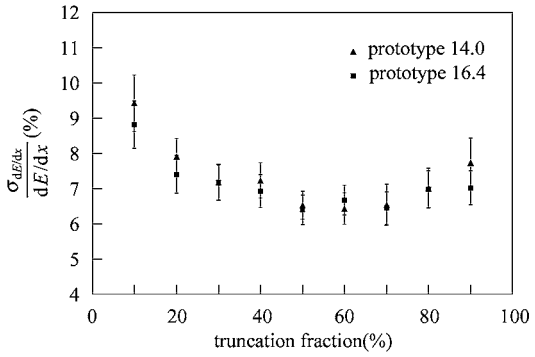

Fig.5. The dE/dx resolution as a function of the truncation fraction.

The dependence of the dE/dx resolution of the two chambers on the number of samples is studied by combining consecutive events. Fig.6 shows the results with the truncation fraction of 60%. The improvement of the dE/dx resolution with the increase of the samples is less than $N^{-0.5}$ as expected from a simple Gaussian, where N is the number of samples. It is due to the long tail of the Landau distribution of dE/dx. The dE/dx resolution of the prototype 16.4 is better than that of the prototype 14.0 with the same number of samples. It is consistent with the expectation, as the sampling length (cell size) of the prototype 16.4 is longer than that of the prototype 14.0. But with the same total sample depth, the resolution of the prototype 14.0 is better than that of prototype 16.4, due to the larger number of samples of the prototype 14.0. It indicates that the contribution of the number of samples to dE/dx resolution is larger than that of the single sample length. Nevertheless both of the dE/dx resolutions using the two cell sizes fulfill the requirement of the BES Ⅲ drift chamber (6%—7%@30—40samples).

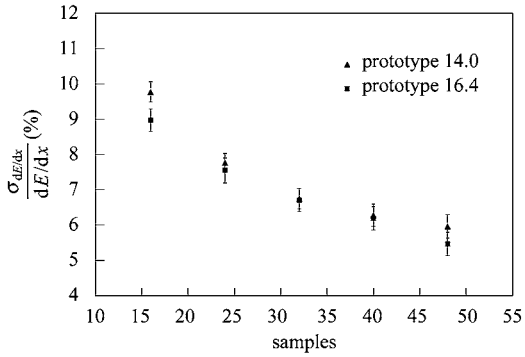

Fig.6. The dependence of the dE/dx resolution on the number of samples.

3.4 Cell efficiency

The dependence of the cell efficiency of the two chambers on the relative gas gain is shown in Fig.7. The efficiency rises with the increase of the operating voltage. An efficiency over 98% can be obtained for the two chambers. They achieve almost equal efficiency with the same gas gain.

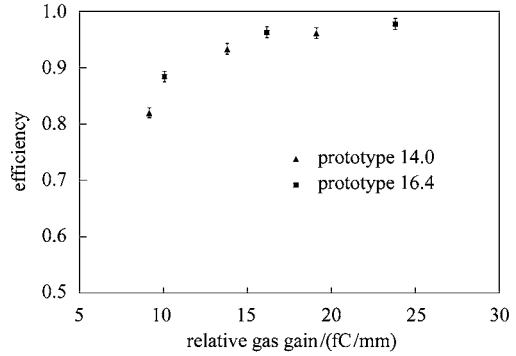

Fig.7. The dependence of the cell efficiency on the relative gas gain.

4 Conclusion

We tested the performance of two prototypes of small-cell drift chamber filled with He/C_3H_8(60/40) with cell sizes of 14.0mm and 16.4mm respectively. The performances of the two drift chambers are almost equivalent.

References

1　Peterson D et al. Nucl. Instrum. Methods, 2002, **A478**:142

2　CHEN Jun et al. Nuclear Electronics & Detection Technology, 2004, **24**: 159 (in Chinese)
(陈君等. 核电子学与探测技术,2004,**24**:159)

3　Jeanne D et al. Nucl. Instrum. Methods, 1973, **A111**: 287

两个不同单元尺寸的小单元漂移室模型的性能研究

刘建北[1,2;1)]　陈昌[1]　陈元柏[1]　金艳[1]　刘荣光[1]　马骁妍[1]　马媛媛[1]
秦中华[1,2]　唐晓[1]　王岚[1]　伍灵慧[1,2]　徐美杭[1]　朱▮萱[1]　朱启明[1]

1 (中国科学院高能物理研究所　北京　100049)
2 (中国科学院研究生院　北京　100049)

摘要　利用宇宙线分别测量了两个单元尺寸为 14mm 和 16.4mm 充 He/C_3H_8(60/40)气体的小单元漂移室模型的性能,包括空间分辨,dE/dx 分辨和单元效率。测量结果表明两个漂移室模型的性能没有明显区别。

关键词　漂移室　小单元　单元尺寸

2004 - 12 - 09 收稿

1) E-mail:liujb@mail.ihep.ac.cn